DSS-13 Ka Receiver Upgrades

Damon Russell,* Ezra Long,† Steven Montanez,† and Michael Young†

ABSTRACT. — The Deep Space Network utilizes its DSS-13 station, located at Goldstone, California, for the research and development of systems deployed within the network. Its unique beam-waveguide architecture allows all receive and transmit electronics to be located within the antenna's pedestal room, greatly easing the installation and evaluation of new hardware. One of the existing receiver electronics packages at DSS-13 is a Ka-band system, originally commissioned for measurements of the cosmic microwave background. This receiver had a system noise temperature of approximately 40 K, which was higher than expected and limited its usefulness to the radio science community. In this article, we report on a number of improvements to the receiver, which have resulted in a 10 K reduction in its system noise temperature and a 2 GHz broadening of its bandwidth.

I. Introduction

DSS-13 is a 34-m beam-waveguide antenna located at Goldstone, California, and used for Deep Space Network (DSN) research and development. Its pedestal room houses a number of cryogenic receiver packages at the common DSN communications bands. It also contains several broader-band receivers, used primarily by the radio astronomy community. The Ka-band (26.5–40 GHz) receiver, described in this article, is one such receiver — shown in Figure 1 — and was first built for cosmic microwave background (CMB) measurements. The receiver's design imposed several limitations to its noise and bandwidth performance, however, limiting its usefulness. This article documents the characterization of the receiver, as well as the upgrades made to the unit that ultimately widened its bandwidth 1–2 GHz and improved its noise temperature by as much as 10 K.

II. Baseline Performance

Microwave radiation collected by the 34-m antenna is guided into the pedestal room where it is channeled into the Ka receiver's feedhorn by a primary and secondary reflector, as shown in Figure 2. The incoming signal is then passed into the cryostat to a polarizer and orthomode transducer (OMT), yielding left-hand circularly polarized (LCP) and right-hand
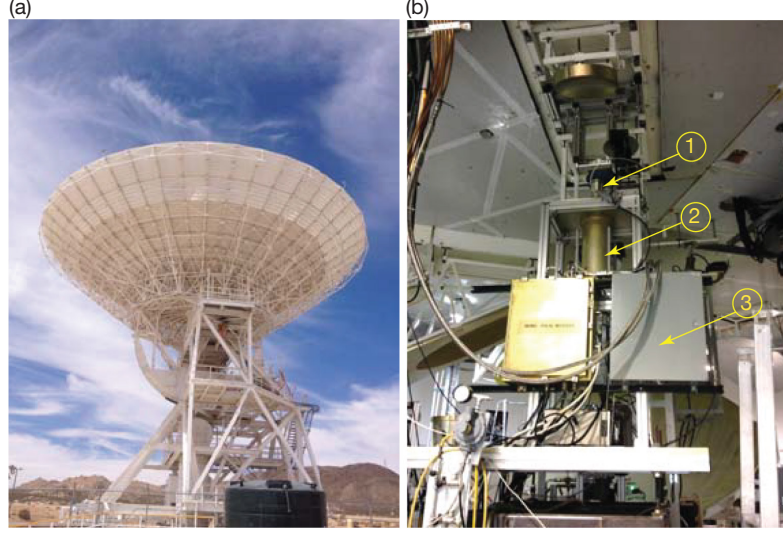

Figure 1. (a) Photograph of DSS-13, 34-m beam-waveguide antenna, Goldstone, California; (b) Ka cryostat in-stalled within the pedestal room of DSS-13: ① Ka feed, ② cryostat, and ③ downconverter electronics box.

circularly polarized (RCP) outputs, which are then amplified. The amplified LCP and RCP signals are then sent into a downconverter for further amplification and downconversion. The local oscillator (LO) signal of 44 GHz folds the RF spectrum of 28–40 GHz to an inter-mediate frequency (IF) of 4–16 GHz. Substantial work on the downconverter was completed several years ago, at which time it was shown to have adequate performance. It was there-fore not included in baseline testing, and was only later evaluated within the system once upgrades to the cryostat were completed.

A. DSS-13

Baseline measurements at DSS-13 were conducted on December 18, 2012. A dichroic plate was originally mounted immediately before the secondary reflector shown in Figure 2, but was determined to dramatically increase the system noise temperature, T_{amw}, and was there-fore removed for all subsequent measurements. T_{amw} is given by Equation (3), following the conventional DSN noise contribution definitions described in [1] and illustrated in Figure 3:

$$T_{amw} = T_{ant} + T_{e1} \tag{1}$$

$$= T_{ant} + T_{rx} + T_{feed} + T_f \tag{2}$$

$$= T_{ant} + T_{rx} + T_{feed} + \frac{T_{be}}{G_{rx}}, \tag{3}$$

where the subscript "1" in T_{e1} refers to the reference plane immediately before the feed mounted to the receiver's cryostat, and "2" to the reference plane immediately after the feed. T_{ant} is composed of antenna spillover[1] and other non-idealities. The simplifying

---

[1] Spillover is itself a function of antenna pointing. The measurements presented here were all made with the antenna pointed at zenith.
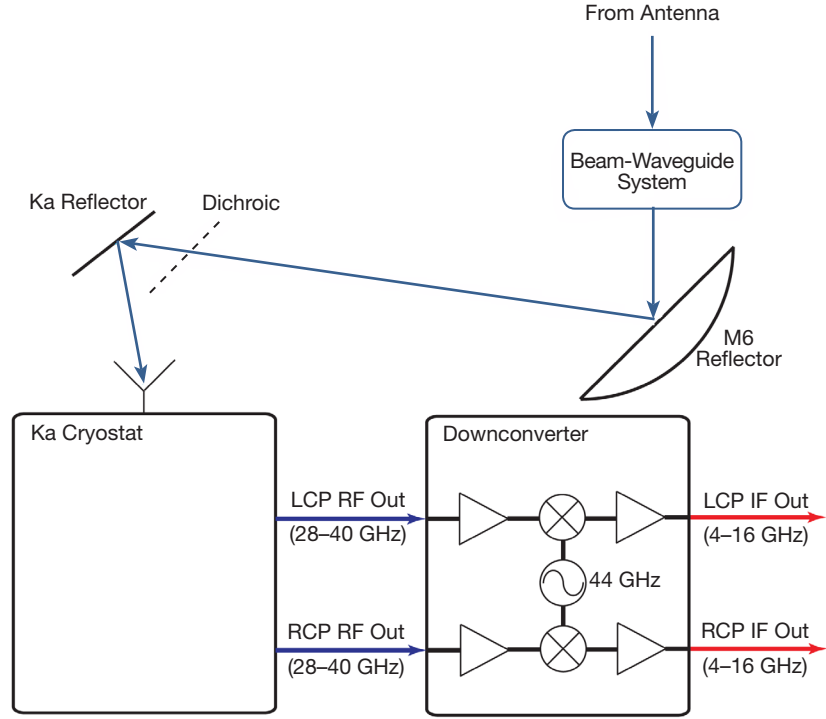
Figure 2. System diagram of the Ka receiver package within the pedestal room. Radiation from the 34-m antenna is guided into the pedestal room where it is reflected off the room's M6 and Ka reflectors into the receiver's feedhorn. The existing dichroic filter was found to severely limit the bandwidth and was removed for all measurements presented here.
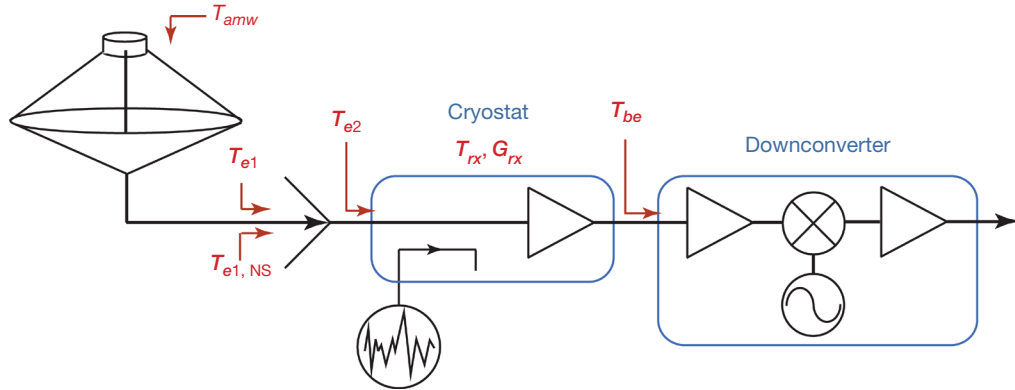

Figure 3. Definition of system noise terms. Although only one channel is shown, the Ka-band cryostat has both LCP and RCP outputs. This is notated by the subscripts LCP, RCP in the measurements to follow (i.e., $T_{e1,RCP}$).

assumption has been made in Equation (3) that all antenna and subsequent beam-wave-guide losses have been lumped into T_{ant}. During baseline tests at DSS-13, T_{e1} was evaluated independently by Y-factor measurements using ambient (~ 300 K) and cold (LN_2 ~ 77 K) loads placed directly in front of the feed (item ① in Figure 1). As these measurements are ratioed, knowledge of the gain is not required,[2] and allows T_{e1} to be determined for the receiver's LCP and RCP channels.

$$Y_{e1} = \frac{P_{LOAD,AMB}}{P_{LOAD,COLD}} \tag{4}$$

$$= \frac{T_{LOAD,AMB} + T_{e1}}{T_{LOAD,COLD} + T_{e1}}$$

$$T_{e1} = \frac{T_{LOAD,AMB} - YT_{LOAD,COLD}}{Y_{e1} - 1} \tag{5}$$

where $P_{LOAD,AMB}$ and $P_{LOAD,COLD}$ are the power measurements from the hot (~ 300 K) and cold (~ 77 K) loads, respectively. Following determination of T_{e1}, T_{amw} is measured by a sub-sequent power measurement with the antenna pointed at zenith. This measurement, P_{SKY}, is referenced against the $P_{LOAD,AMB}$ measurement made earlier:

$$Y_{amw} = \frac{P_{LOAD,AMB}}{P_{SKY}} \tag{6}$$

$$\approx \frac{T_{LOAD,AMB} + T_{e1}}{T_{sky} + T_{amw}}$$

$$T_{amw} \approx \frac{T_{LOAD,AMB} + T_{e1} - YT_{sky}}{Y_{amw}} \tag{7}$$

Assuming relatively dry and clear conditions, the effective sky temperature, T_{sky}, can be determined as a function of frequency, altitude, pressure, and humidity using the atmospheric noise model developed by Slobin [2]. All power measurements presented here were made using an Agilent E4448A spectrum analyzer, using a 4-MHz resolution bandwidth and 100-Hz video bandwidth. The downconverter was not utilized during these baseline measurements at DSS-13. Referring to Figure 3, all noise contributions after the low-noise amplifier (LNA), (T_{be}), referred back to the feed, are the follow-up noise, T_f:

$$T_f = \frac{T_{be}}{G_{rx}}.$$

As a result of the measurement configuration, T_f is solely composed of the spectrum analyzer's contribution. Measured results of T_{amw} are shown in Figure 4, where it can be seen that the mean T_{amw} is approximately 40 K for RCP and 37 K for LCP over a bandwidth of 28.5 to 34 GHz. There was about 5 K of ripple on the measured values of T_{amw}. Tests with the system noise source turned on and off (the system's noise source is external to the receiver's

---

[2] Individual power measurements take several tens of seconds to complete. The effects of gain fluctuations ($\Delta G/G$) are therefore ignored.
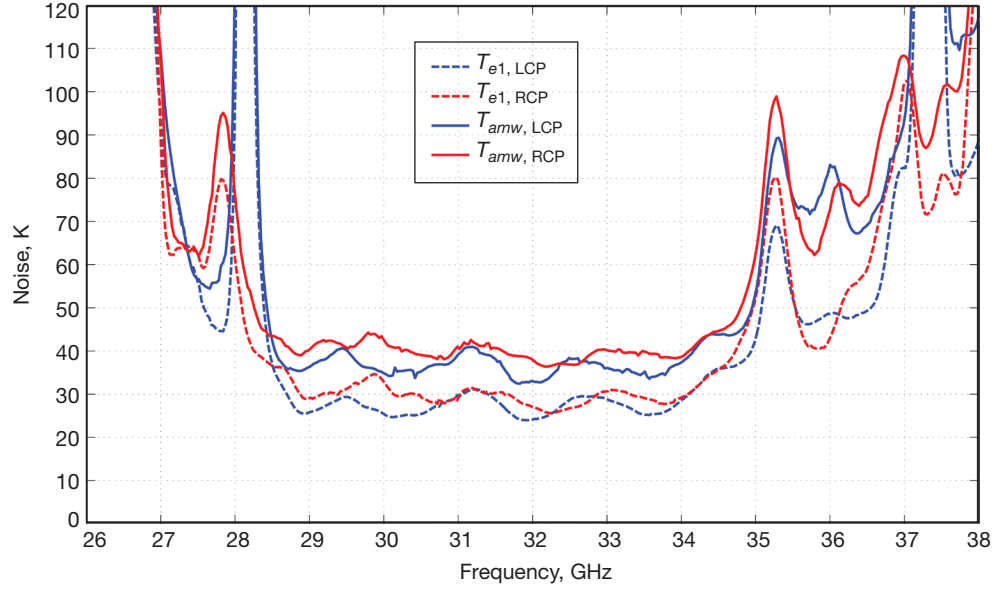
Figure 4. Baseline measurements of T_{amw} measured at DSS-13 and T_{e1} measured at JPL at the top of building 238.

cryostat) produced no change in the measured power output of the system. The cryostat internal temperature sensors, placed on the RCP LNA, LCP LNA, first stage cold head, and second stage cold head measured 20 K, 20.5 K, 450 K, and 66 K, respectively. The LNA temperatures were about 5–8 K higher than expected; the LNAs in most DSN cryostat systems operate below 20 K. The 450 K temperature on the second stage of the cold head indicated that this sensor was damaged.

B. JPL Rooftop Testing

Following receipt of the receiver and downconverter electronics at JPL, testing of T_{e1} was completed on the rooftop of building 238. In place of the LN_2 load, utilized to determine T_{e1} at DSS-13, a cold-sky measurement was made instead. The test setup for this measurement can be seen in Figure 5(b). These results agreed well with those made at DSS-13 and served as the baseline for improvements to the system. Measurements of T_{e1} are shown in Figure 4, and reveal the same ripple structure as observed during DSS-13 tests. Mean T_{e1} was approximately 30 K for RCP and 27 K for LCP over the same 28.5–34 GHz bandwidth. These results revealed that T_{ant} contributes $\approx$ 10 K to T_{amw}. During these tests, it was also observed that the external noise source did not draw any current from its +28 V supply, explaining the lack of any measurable deflection when the noise source was cycled on and off during earlier tests at DSS-13.
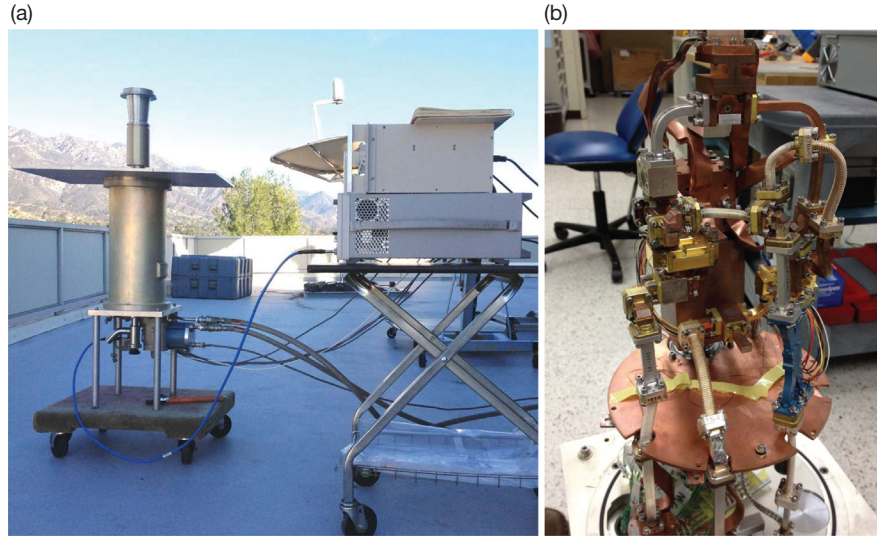
Figure 5. (a) Rooftop testing of Ka cryostat on the roof of building 238 at the Jet Propulsion Laboratory, Pasadena, California. Measurements were made of cold sky (shown) and of a warm load (a large piece of absorber placed over the feedhorn). (b) Ka cryostat with vacuum jacket removed.

III. Modifications

Following baseline measurements, the cryostat was disassembled and inspected. It is shown with its vacuum jacket removed in Figure 5(b). During disassembly, inadequate heat strapping of the LNAs and input polarizer was discovered; the most likely reason the LNAs had only cooled to ~ 20 K. The architecture for the new system is shown in Figure 6. It consists of modifications to the input transition, polarizer, LNAs, cryogenics, and power supply, which are discussed in the following sections. The Product Data Management System (PDMS) drawing numbers documenting the new hardware developed for the system are provided in Table 1.

A. Input and Polarizer

The input of the LNA is a WC-34 (ø.34 inch) waveguide, including a quartz vacuum window and a thermal isolator choke gap section of waveguide. This feeds into a septum polarizer,[3] which first transforms to 0.22-inch-square waveguide and then splits the circularly polarized signal into LCP and RCP WR-28 outputs. The quartz window was removed and replaced with a 0.005-inch Kapton window similar in design to that seen on most other LNA systems in the DSN. In addition, a small, low-loss section of foam was added to the throat of the thermal isolator, which acts as an infared block and reduces the chance of condensation on the vacuum window. It was found that the groove in the waveguide, into which the quartz window rested, caused a resonance and thus a noise spike around 28 GHz. The quartz window contributed partially to the passband noise ripple due to the

---

[3] Although the name is misleading, the septum polarizer provides both polarizer and OMT functions.
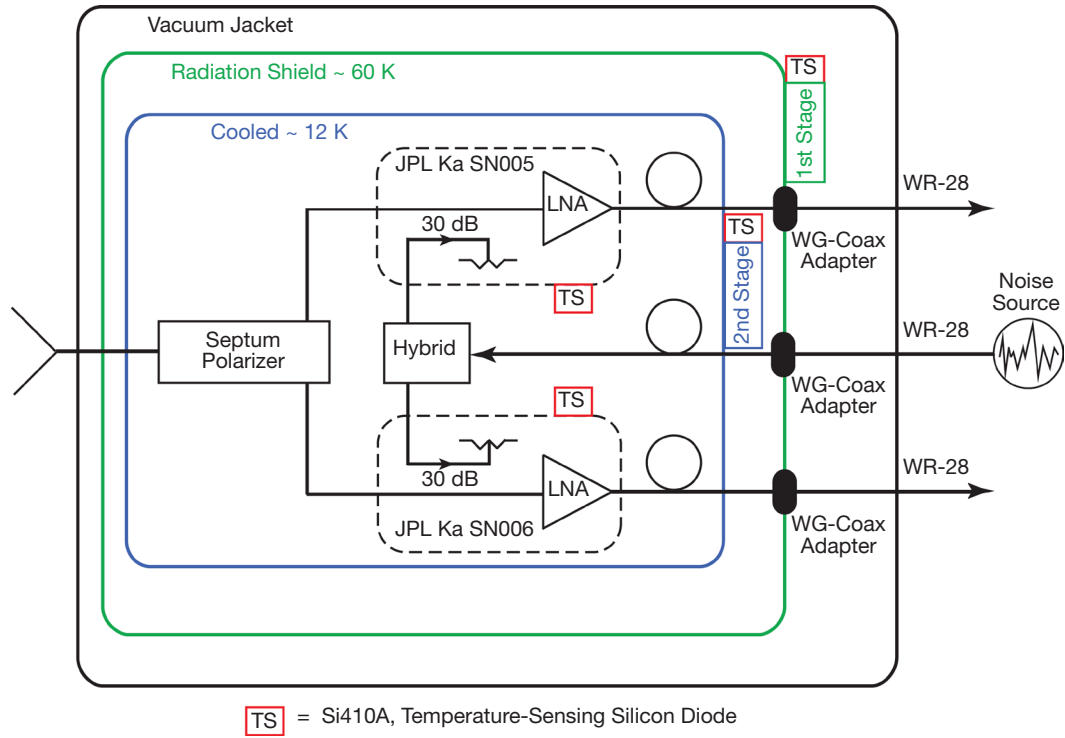
Figure 6. System diagram of the modified receiver.

┌─────┐
│ TS │ = Si410A, Temperature-Sensing Silicon Diode
└─────┘

Table 1. DSS-13 Ka PDMS drawing numbers.

Drawing Number	Title
9629327	Ka Power Supply
9629561	Ka Cryostat Harness
9629562	Ka Power Supply to Cryostat Harness
9629563	Ka Supply Schematic

poor match it presented. The use of Kapton introduces a small vacuum leak of 5×10^{-5} Torr-cc/s; this is seen on other LNA systems within the DSN that use such a vacuum window and it corresponds well to published results [3]. Both the WC-34 and the 0.22-inch-square guide have modes around 26.5 GHz; the square waveguide also has an additional mode at 37.5 GHz. These modes correspond to the peaks in the noise temperature observed in measured data. By analyzing and redesigning the input and polarizer concurrently, the usable bandwidth of the system could be increased and peaks in noise temperature removed.

B. Low-Noise Amplifiers

The existing system used LNAs built by the National Radio Astronomy Observatory (NRAO) using high-electron-mobility transistors (HEMTs) from the "cryo-3" wafers. These LNAs (serial numbers AM007 and AM006) were removed from the receiver and tested within the Ka cryogenic testbed operated by the JPL Communications Ground Systems Section. In order

to emulate the bias conditions as closely as possible, a custom set of cables was fabricated that allowed use of the existing power supply with the testbed. The measured results, at a physical temperature of 12.8 K, are shown in Figure 7. The NRAO LNAs contain integrated light-emitting diodes (LEDs), in principle used to free carriers from traps within the HEMTs. Noise measurements with the LEDs biased at 5 and 8 mA of current revealed no reduction in noise temperature, however. AM007, contained within the RCP channel of the receiver, had an average noise temperature of 20 K from 28–34 GHz. AM006 had better performance, with a mean noise temperature of 16.5 K across the same frequency range.
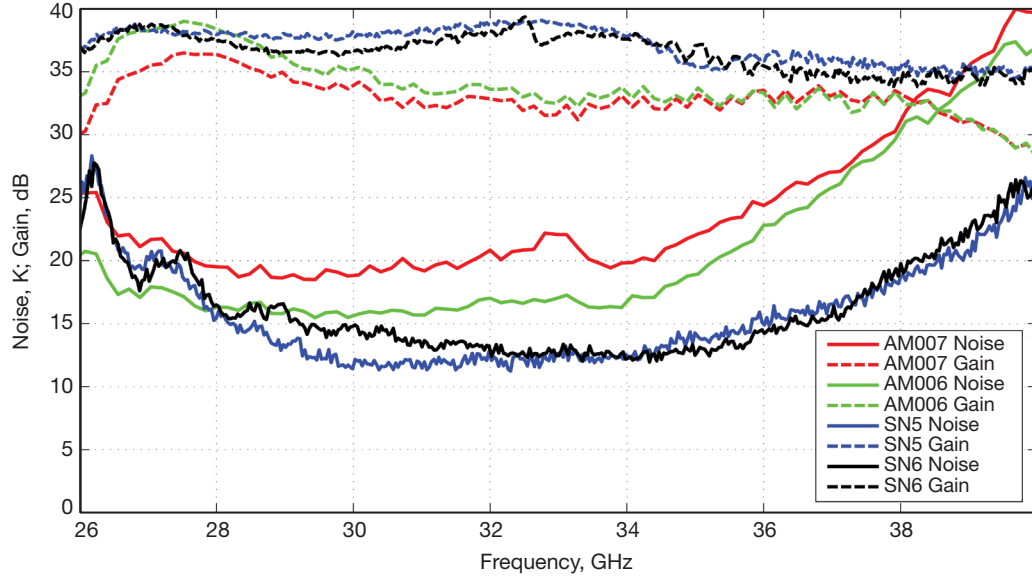

Figure 7. Cryogenic noise temperature and gain for the original LNAs used within the Ka receiver, manufactured by NRAO, and the retrofitted LNAs manufactured by JPL. The NRAO amplifiers, serial numbers AM007 and AM006, were in the RCP and LCP channels, respectively. JPL amplifiers SN05 and SN06 were placed in the RCP and LCP channels, respectively, of the modified receiver.

The NRAO amplifiers were replaced with Ka LNAs sourced from the DSN's array project [4]. These LNAs had noise temperatures of 12–15 K, roughly 5–8 K better than the existing NRAO amplifiers. They also have about 5 dB more gain, thus reducing the noise contribution from the downconverter and subsequent electronics. In addition, these amplifiers contain an integrated 30-dB coupler, greatly simplifying their integration within the receiver. The measured noise of the two DSN LNAs integrated within the modified receiver (serial number 05 was integrated within the RCP channel and 06 within the LCP channel) is shown in Figure 7 as well. These measurements confirm the 5–8 K expected improvement in noise temperature from the new LNAs.

C. Cryogenics

The internal cryogenics, heat straps, and cabling had a variety of problems and were completely reworked. Initial tests of the LNA system showed physical temperatures of ~ 20 K; after modifications, the system now operates around 12 K. The system has three WR-28

waveguide ports; two LNA outputs and one noise input port. The Kapton vacuum windows for the three WR-28 ports were replaced with the current DSN Ka-band foam vacuum windows [5]. The thermal isolators on the three waveguide ports were replaced with 5-inch thin-wall stainless steel waveguide sections with a silver flash that are thermally sunk to the first stage of the cryocooler. The waveguides transition to flexible coax to attach to the internal components; these coaxes could be replaced with semi-rigid coaxes if any gain stability issues develop. The noise input port is split by a 90-deg hybrid before being fed into the LNA coupler ports. New heat straps to all the cooled components were fabricated. The internal bias and temperature diode cabling was completely remade with Lakeshore[4] Quad-Twist cryogenic wire (part number QT-36) to reduce the thermal load. Four new DT-470 temperature diodes from Scientific Instruments[5] were installed in the system.

D. Power Supply

For this project, a new four-channel power-supply card was designed. It is loosely based on the existing HEMT DC supply used by the DSN, and those manufactured by the California Institute of Technology[6] for the radio astronomy community. To simplify the design, the drains are operated at constant voltage; there is no servomode whereby the drain current can be fixed. Drain and gate voltages are adjusted via onboard potentiometers. Buffers are included for monitoring both the gate and drain voltages. To scale the drain and gate currents up to voltages that are easily monitored, these signals are each amplified with a two-opamp instrumentation amplifier. The transducer gains for the gate and drain current monitors are 68.2 µA/V and 5.4 mA/V, respectively. Since the gate leakage currents are on the order of several µA for low-noise HEMTs, the gate current monitor may be zeroed through a potentiometer, removing the offset introduced by the input bias currents from the instrumentation amplifiers (~ 200 nA). The schematic and printed circuit board (PCB) for the four-channel board are documented in PDMS under drawing number 9629327; see Figure 8.

The power supply card is fed by an Acopian[7] DB5-25 AC/DC (± 5 V, 250 mA) power supply. To suppress the effects of transients when the unit is turned on and off, a Schottky/Zener diode network is placed between the Acopian outputs and power supply cards' DC inputs. The HEMT outputs from the supply cards are routed to a 64-pin circular connector, mounted on the front panel of the supplies enclosure. Monitor outputs are routed to a 25-pin, D-sub female connector, also mounted to the front panel. The pin-out for the 25-pin monitor is listed in Table 2, along with the monitor readings taken upon installation of the Ka receiver at DSS-13 on May 21, 2013. PDMS drawing number 9629562 documents the wiring of the power supply enclosure, including the pin-out of the 64-pin circular connector

Although power supply transient effects were mitigated through the use of the diode network mentioned above, future revisions of the power supply card should include the addition of transient-suppression diodes at the HEMT supply outputs. A simple solution for the gates would be an anti-parallel set of diodes, each set consisting of one to two 1N4148

---

[4] Lakeshore Cryotronics, 575 McCorkle Blvd., Westerville, OH 43082 U.S.A.

[5] Scientific Instruments, 4400 West Tiffany Dr., West Palm Beach, FL 33407 U.S.A.

[6] California Institute of Technology, 1200 East California Blvd., Pasadena, CA 91125 U.S.A.

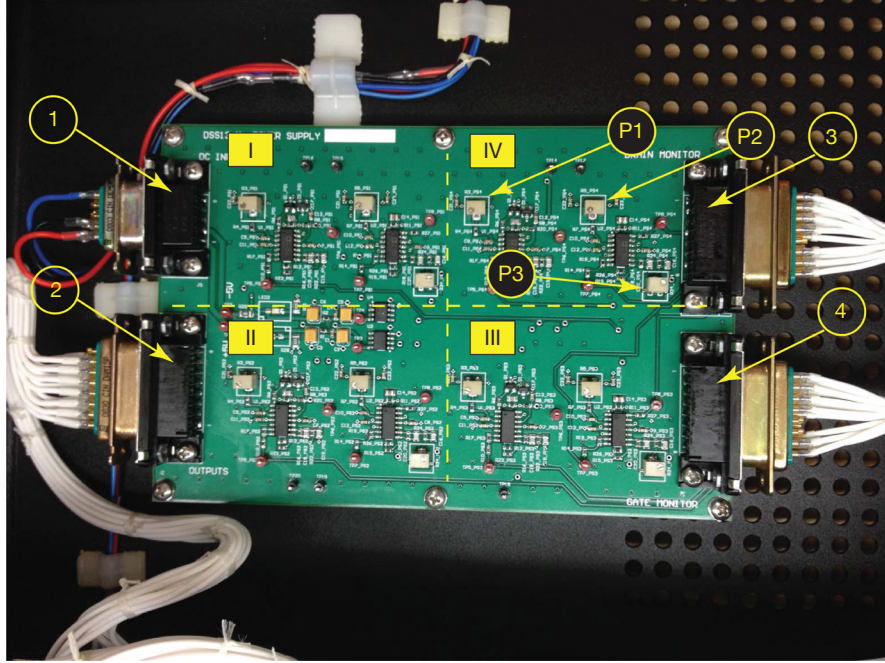[7] Acopian Technical Company, P.O. Box 638, Easton, PA 18044 U.S.A.

Figure 8. Four-channel PCB for biasing of the LNAs. The four channels are (I) RCP stage 1, (II) RCP stage 2, (III) LCP stage 1, and (IV) LCP stage 2. Potentiometers for each channel are for adjustment of (P1) drain voltage, (P2) gate voltage, and (P3) gate current readout offset. Connectors are ① input ± 5 V, ② LNA drain, gate, and return lines, ③ gate monitor, and ④ drain monitor.

diodes[8] shunted between the gate outputs and ground. Such changes will provide an additional layer of protection for LNAs. This is not a concern for the JPL LNAs currently employed in the receiver, as they have their own internal diode-protection networks.

E. Assembly

Following modification of each of the receivers' elements, the cryostat was reassembled. Figure 9 shows the completed system. New heat straps and brackets were fabricated from electrolytic tough-pitch (ETP) copper.[9] Indium foil was placed between all interfaces between heat straps and their cold plates, along with the attachment points to the first and second stages of the cryocooler. The stand supporting the polarizer was also remade from nylon and G-10, to ease reassembly of the unit and to simplify the mechanical design.

IV. Performance

Tests of the refurbished receiver were conducted initially on the roof of building 238 at JPL and later at DSS-13. Unlike the baseline measurements, tests with the refurbished system

---

[8] One 1N4148 diode would clamp at ~ 0.6 V, two in series at ~ 1.2 V.

[9] ETP copper has similar performance to oxygen-free high-thermal-conductivity copper (OFHC) but is more readily available.

Table 2. Drain and gate monitors. Multiplying the monitor output by the monitor response yields the respective LNA bias setting. Settings were recorded on May 21, 2013.

Pin Number	Net Name	Output Voltage, V	Monitor Response
1	V_{DRAIN} , RCP Stage 1	0.795	1V/V
2	I_{DRAIN} , RCP Stage 1	2.672	5.4 mA/V
3	Ground	0	—
4	V_{DRAIN} , LCP Stage 1	0.676	1V/V
5	I_{DRAIN} , LCP Stage 1	2.766	5.4 mA/V
6	Ground	0	—
7	Ground	0	—
8	Ground	0	—
9	V_{GATE} , RCP Stage 2	0.168	1V/V
10	I_{GATE} , RCP Stage 1	0.037	68 µA/V
11	Ground	0	—
12	V_{GATE} , LCP Stage 2	0.138	1V/V
13	I_{GATE} , LCP Stage 2	–0.014	68 µA/V
14	Ground	0	—
15	V_{DRAIN} , RCP Stage 2	0.903	1V/V
16	I_{DRAIN} , RCP Stage 2	2.230	5.4 mA/V
17	Ground	0	—
18	V_{DRAIN} , LCP Stage 2	0.903	1V/V
19	I_{DRAIN} , LCP Stage 2	2.194	5.4 mA/V
20	V_{GATE} , RCP Stage 1	0.167	1V/V
21	I_{GATE} , RCP Stage 1	0.039	68 µA/V
22	Ground	0	—
23	V_{GATE} , LCP Stage 1	0.223	1V/V
24	I_{GATE} , LCP Stage 1	0.059	68 µA/V
25	Ground	0	—

included the downconverter within the signal chain. Measurements were conducted in the same fashion as described in Section II. The only exception was the addition of measurements for evaluation of the noise source temperature, referred to the input of the system. Following measurement of T_{RX} for LCP and RCP channels using ambient and sky measurements, the noise temperature of the external noise source was measured by firing the noise source with the receiver pointed at cold sky. While this measurement could have also been made with the receiver looking at an ambient load, the smaller change in Y-factor results in higher uncertainty [6]. The noise source's temperature, for RCP and LCP channels, is determined from the Y-factor measurements using the following relations:

$$Y_{e1,NS} = \frac{T_{SKY} + T_{e1,NS} + T_{e1}}{T_{SKY} + T_{e1}}$$
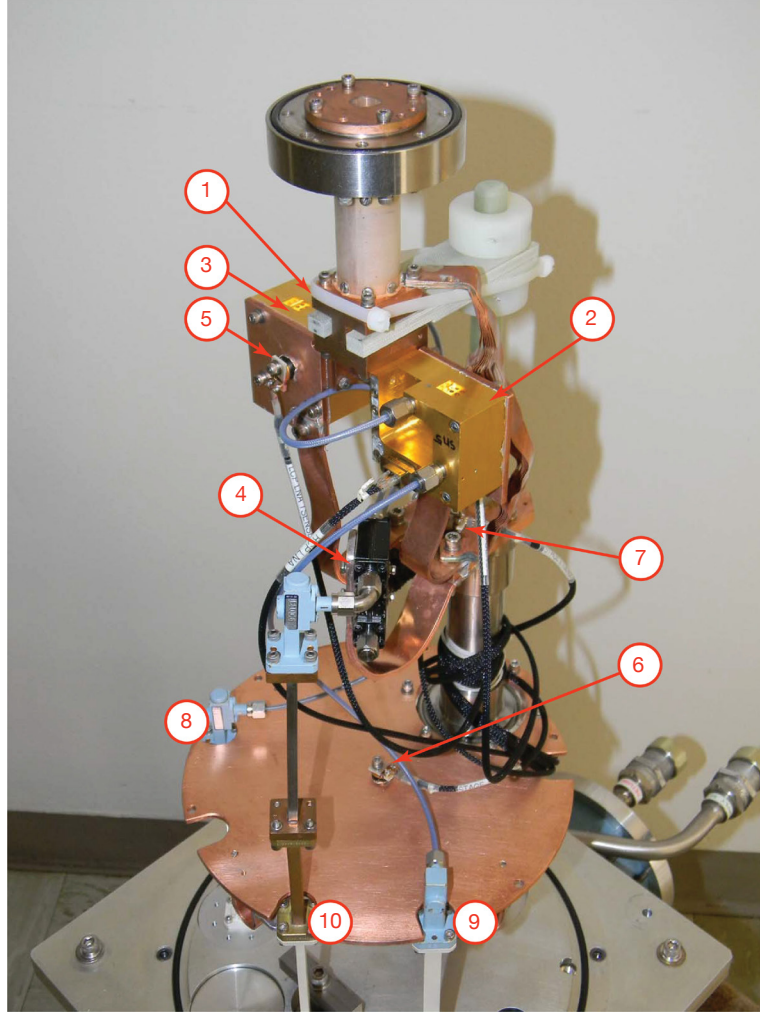
$$T_{e1,NS} = (Y_{e1,NS} - 1)(T_{SKY} + T_{e1}) \tag{8}$$

Figure 9. Modified Ka system with vacuum jacket removed: (1) Input polarizer, (2) RCP LNA, (3) LCP LNA, (4) 90-deg hybrid 3-dB splitter, (5) LCP LNA temperature sensor, (6) first-stage temperature sensor, (7) second-stage temperature sensor, (8) LCP output, (9) RCP output, and (10) noise source input. Note that the modified system is much cleaner in appearance than the original system shown in Figure 5.

A. JPL Rooftop Testing

Measurements of the T_{RX} are shown in Figure 10, compared with measurements made prior to modifications. These measurements reveal an improvement of 1–2 GHz in the bandwidth and removal of the majority of the ripple contained within the noise temperature. The noise temperature improved by 5–10 K over the majority of the band. Improvements to the system were also revealed by the drop in measured physical temperatures within the receiver's cryostat. Temperatures of 13.06, 12.96, 71.10, and 13.03 K were measured for the RCP LNA, LCP LNA, first-stage cold plate, and second-stage cold plates, respectively. Similar LNA and second-stage cold-plate temperatures reveal the benefits from the new heat strapping and cabling incorporated into the rebuilt system.
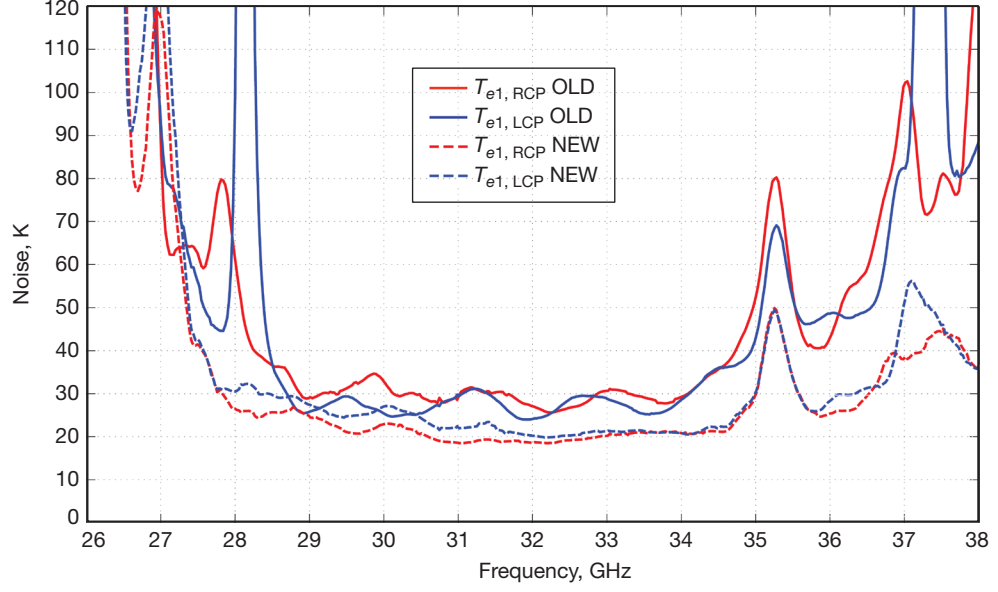
Figure 10. Measurements of T_{e1} atop building 238 at JPL.

Following measurement of T_{e1}, T_{NS} was measured for both RCP and LCP channels, as previously described. The measured results are shown in Figure 11, revealing a mean temperature of 30 K for RCP and 18 K for LCP. The difference in noise source temperature between RCP and LCP channels is attributed to the differences in the coaxial cabling between channels within the cryostat and to the performance of the couplers integrated within the LNAs.

B. DSS-13 Measurements

Measurements at DSS-13 on May 21, 2013, revealed the same improvements to the noise temperature and bandwidth as measured at JPL. Figure 12 shows the measurements of T_{amw} plotted against the earlier baseline measurements. The 5–8 K improvement in noise temperature, reduction in ripple, and 1–2 GHz increase in system bandwidth are evident.

V. Future Work

Future work on the DSS-13 Ka system can be broken into three areas: receiver enhancement, back-end electronics development, and system monitoring. With regards to receiver enhancement, the bandwidth of the system is limited by the input transition/polarizer and the LNAs in about equal measure. Any significant (1–2 GHz) improvement to the bandwidth will require work on both elements. The input transition/polarizer may be the more challenging of the two. The current bandwidth of ~ 20 percent is fairly typical of what can be achieved with a septum polarizer. Bandwidths of ≥30 percent may be possible with iris-loaded waveguide polarizers [7], at the cost of a physically larger and more complex structure. Such polarizers would also require an OMT to properly separate the RCP and LCP signals. Several options exist for enhancements to the LNA performance. Low Noise Fac-
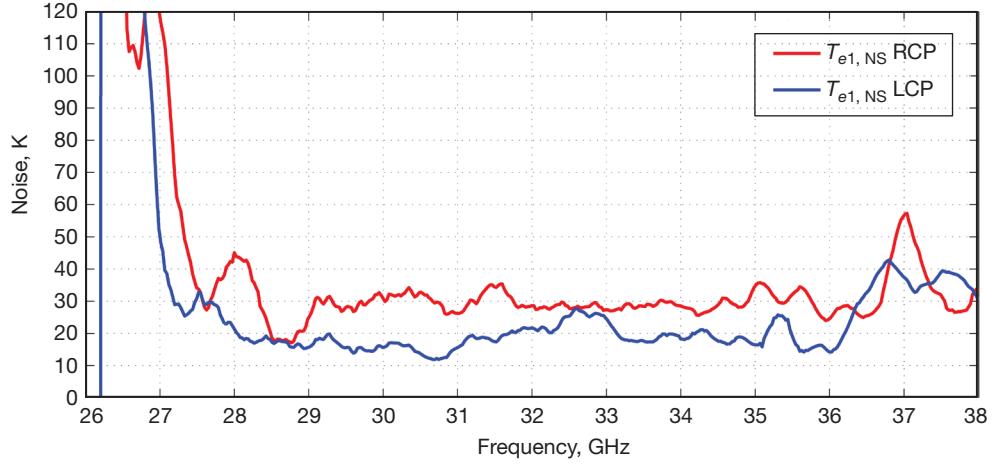
Figure 11. Noise source temperatures referenced to the input of the receiver's feed (reference plane 1 in Figure 3) measured on top of building 238 at JPL. The external noise source's power is split within the cryostat and injected to a coupler integrated within each LNA. This results in an effective noise source temperature for both LCP and RCP channels.
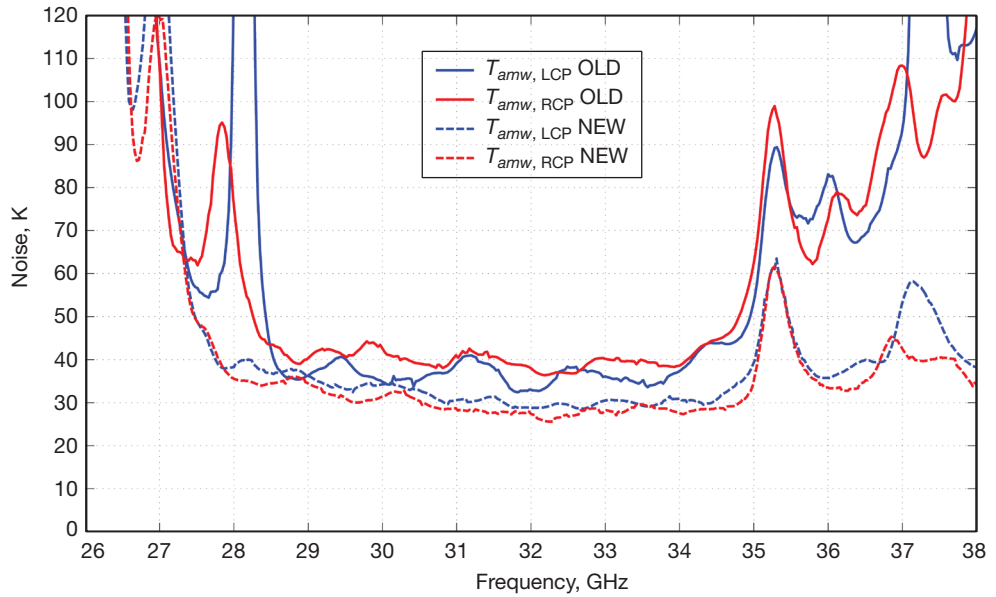

Figure 12. Measurements of T_{amw} at DSS-13.

tory[10] offers a cryogenic Ka-band (part number LNF-LNC22-40WA) LNA with ≈ 13 K noise temperature from 26–34 GHz. Alternatively, JPL has began evaluation of a Northrop Grumman Space Technology (NGST)–fabricated 35-nm indium phosphide (InP) Ka monolithic microwave integrated circuit (MMIC) that shows promising cryogenic noise performance. Improvements to the noise source's temperature stability may be achieved with integration of the noise source inside the receiver's cryostat. Noise diodes from companies such

---

[10] Low Noise Factory, AB., 37 Frölundagatan, Mölndal 43144, Sweden.

as Metelics[11] have been shown to operate well at cryogenic temperatures [6]. Mounting this cryogenic noise source to the cold plate of the second stage would improve the noise source's stability, as the stage temperature only deviates ~ hundreds of mK during operation. In addition, the range of noise diode brightness temperatures would also be increased, as the lossy, thermally insulating waveguide and coax interconnects would no longer be necessary. One could envision the development of a cryogenic noise source module with multiple outputs, each with a different noise brightness temperature. Such a module, inherently stable, would be useful not only for receiver noise calibration, but also for calibration of receiver linearity.

The system's downconverter outputs an IF of 6–20 GHz, currently too high to meet the capabilities of broadband digital spectrometers, whose state of the art is currently ~ 10 GHz of bandwidth. With the current configuration of the receiver, the usable bandwidth is approximately 6 GHz wide. It would be extremely useful to develop a second stage of downconversion to mix the current usable IF bandwidth down to frequencies compatible with today's digital spectrometers. Such a capability would also allow the system to be used with products such as the compact, broadband spectrum analyzers from Test Equipment Plus.[12] Connected with a simple PC, 20 MHz of analog bandwidth between 9 kHz and 6 GHz could be digitally sampled and remotely available for analysis.

Monitoring of system parameters such as LNA bias, cryostat temperatures, and vacuum currently must be done within the pedestal room via direct readings. Adapting a DSN cryogenic control/monitor system would allow cryostat temperature and vacuum to be controlled and monitored remotely. The addition of a separate microcontroller, such as the Ethernet-enabled Arduino,[13] would allow LNA bias parameters to be remotely monitored. Such an upgrade would be fairly simple to implement, and could be installed in the existing enclosure for the receiver's power supply.

VI. Summary

Performance enhancements to the DSS-13 Ka receiver package have been presented. Inspection of the unit after baseline testing revealed a number of issues that were addressed with subsequent modifications. The input transition from the feedhorn to the polarizer was found to be limiting the bandwidth and responsible for the ripple observed on the noise temperature. Broader-band, lower-noise LNAs from the DSN array project replaced the existing NRAO-sourced LNAs. A custom power supply was developed for the DSN LNAs and extensively tested. Numerous issues with the heat strapping and cabling inside the receiver were addressed. These combined changes allowed for a 1–2 GHz increase in the bandwidth of the receiver, a 5–10 K reduction in the system noise temperature, and a significant reduction in the noise temperature ripple. The noise source, originally inoperable, was repaired and its input referred noise temperature of 15–30 K measured. Detailed descriptions of the measurements and test setups were presented.

---

[11] Aeroflex/Metelics, 975 Stewart Dr., Sunnyvale, CA 94086 U.S.A.

[12] Test Equipment Plus, 35707 North East 86th Ave., La Center, WA 98629 U.S.A.

[13] http://www.arduino.cc

References

[1] M. Reid, ed., *Low-Noise Systems in the Deep Space Network*, Wiley-Interscience, pp. 13–93, February 2008. Also available online: Deep Space Communications and Navigation Systems Center of Excellence (DESCANSO) Deep Space Communications and Navigation Series, Jet Propulsion Laboratory, Pasadena, California, February 2008. http://descanso.jpl.nasa.gov/Monograph/series10/Reid_DESCANSO_sml-110804.pdf

[2] S. Slobin, "Atmospheric and Environmental Effects," *DSN Telecommunications Link Design Handbook*, Space Link Interfaces 105D, DSN No. 810-005, Jet Propulsion Laboratory, Pasadena, California, September 15, 2009. http://deepspace.jpl.nasa.gov/dsndocs/810-005/

[3] J. dos Santos, "Simple Vacuum Experiments for Undergraduate Laboratories," *Vacuum*, vol. 80, no. 1–3, pp. 258–263, October 2005.

[4] Y. Tang, N. Wadefalk, M. Morgan, and S. Weinreb, "Full Ka-Band High-Performance for InP MMIC LNA Module," *2006 IEEE MTT-S International Microwave Symposium Digest*, vol. 1, pp. 81–84, San Francisco, California, June 11–16, 2006.

[5] M. Britcliffe, T. Hanson, E. Long, and S. Montanez, "High-Reliability Waveguide Vacuum/Pressure Window," *NASA Tech Briefs*, vol. 37, no. 2, p. 34, February 2013.

[6] D. Russell and S. Weinreb, "Cryogenic Self-Calibrating Noise Parameter Measurement System," *IEEE Transactions on Microwave Theory and Techniques*, vol. 60, no. 5, pp. 1456–1467, May 2012.

[7] S. Srikanth, "A Wide-Band Corrugated Rectangular Waveguide Phase Shifter for Cryogenically Cooled Receivers," *IEEE Microwave and Guided Wave Letters*, vol. 7, no. 6, pp. 150–152, June 1997.